CRYSTAL GROWTH & DESIGN

ARTICLE

pubs.acs.org/crystal

Improving the Poor Aqueous Solubility of Nutraceutical Compound Pterostilbene through Cocrystal Formation

Sarah J. Bethune,* Nate Schultheiss,† and Jan-Olav Henck

SSCI, a division of Aptuit, 3065 Kent Avenue, West Lafayette, Indiana, United States

Supporting Information

ABSTRACT: Pterostilbene is a nutraceutical compound being investigated for its ability to form cocrystals with pharmaceutically acceptable coformers to improve its poor aqueous solubility. Cocrystals of a 2:1 and 1:1 stoichiometric molar ratio of pterostilbene with piperazine or glutaric acid were synthesized on a multigram scale and fully characterized including single-crystal X-ray diffraction. Furthermore, both cocrystals were evaluated for physical stability with respect to humidity and temperature as well as kinetic solubility. Each cocrystal displayed remarkable stability, showing no evidence of dissociation across a range of durations, temperatures, and relative humidities. The aqueous concentration of pterostilbene measured over five hours from dissolution of the pterostilbene-piperazine cocrystal was six times higher than the solubility of the single-component pterostilbene. Although X-ray powder diffraction results indicate partial transformation of the pterostilbene-piperazine cocrystal to pterostilbene after 5 h, this increase in concentration was sustained throughout the dissolution experiment. Within 5 min of slurrying the pterostilbene-glutaric acid cocrystal in water, precipitation of pterostilbene was observed; thus no dissolution data under these conditions were obtained.

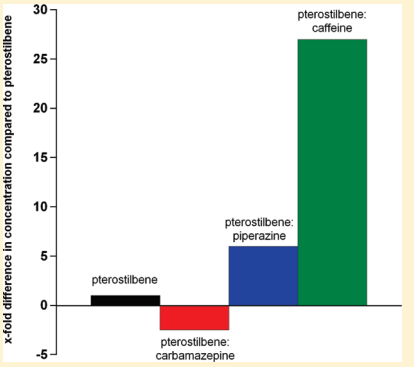

INTRODUCTION

Pterostilbene, a naturally occurring analog of resveratrol, is classified as a nutraceutical compound[1] with its greatest abundance found in a variety of different berries.[2] In a number of animal studies, pterostilbene was found to lower cholesterol, regulate blood sugar levels, and be as effective as resveratrol as an anti-carcinogenic agent.[3] Furthermore, initial studies on comparative pharmacokinetics of pterostilbene and resveratrol resulted in the former showing enhanced lipophilicity and membrane permeability and thus greater bioavailability over the latter.[4]

Although pterostilbene has shown some promising initial pharmacokinetic studies, a potential drawback is its extremely low aqueous solubility, approximately 21 μg/mL.[5] A common approach to increasing the solubility of a poorly soluble compound, especially in the pharmaceutical and agrochemical industry, is through the formation of a crystalline salt. Unfortunately pterostilbene is not chemically amenable for such a modification. Thus, another potential option is the formation of a cocrystal (or multicomponent crystal) where the individual components are connected by noncovalent interactions, typically hydrogen bonds.[6] One benefit in forming cocrystals is that it allows for changes to be made to the crystal structure of the parent molecule without introducing chemical modifications, which could change the bioactivity profile of the active pharmaceutical ingredient (API). Cocrystals have been shown to be effective in altering the physicochemical properties of APIs, particularly aqueous solubility and dissolution rates.[7]

As a cocrystal dissolves, the concentration in solution may be supersaturated, saturated, or undersaturated with respect to the individual components. Cocrystal dissolution that results in undersaturated concentrations of individual components leads to solution stability. Cocrystal dissolution that leads to supersaturated concentrations of one or both components may result in precipitation of the component(s), and therefore the cocrystal is not stable in solution. Recent studies on a homologous series of carbamazepine cocrystals have been published relating aqueous stability and kinetic solubility.[8] Coformers with high aqueous solubility, such as glutaric, malonic, and glycolic acids, resulted in cocrystals that were unstable in water; as the cocrystal dissolved, the concentration of carbamazepine in solution increased beyond the solubility of carbamazepine dihydrate and thus precipitated. Coformers with lower aqueous solubility, such as fumaric and 1-hydroxy-2-naphthoic acid, often resulted in stable cocrystals in water, and no precipitation was observed.

In a recent study, we demonstrated the ability of pterostilbene to form cocrystals with the APIs carbamazepine and caffeine and the aqueous solubility of each cocrystal was measured. The caffeine cocrystal resulted in approximately 27-fold increase in concentration (kinetic, sustained for at least 5 h) in comparison to pterostilbene.[9] Within this study, we opted to screen pterostilbene with pharmaceutically acceptable coformers that possess relatively high aqueous solubilities[10] with the intentions of using cocrystals to increase the poor solubility profile of pterostilbene.

Received: December 3, 2010
Revised: April 15, 2011
Published: May 17, 2011

Scheme 1. Molecular Structures of Pterostilbene, Piperazine, and Glutaric Acid (Left to Right)

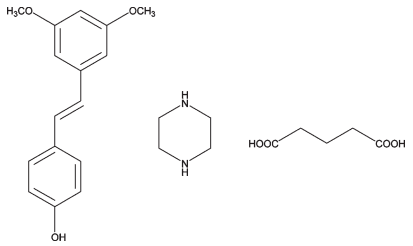

In this paper, we describe the synthesis and characterization of two pterostilbene cocrystals with coformers piperazine and glutaric acid, Scheme 1. Piperazine is a pharmaceutically accepted basic salt former but also has pharmacological activity as an anthelmintic.[11] Although glutaric acid is not listed as pharmaceutically acceptable according to Stahl and Wermuth,[11] the toxicity profile of glutaric acid falls within the range of several pharmaceutically acceptable compounds that are included. Both cocrystals were generated on a multigram scale and characterized by X-ray powder and single-crystal diffraction, differential scanning calorimetry (DSC), thermogravimetric analysis (TGA), and ^{1}H NMR. To evaluate the physical stability, accelerated tests were conducted over a number of temperatures, humidities, and durations. Additionally, powder dissolution was studied for both cocrystals to evalute their ability to increase the poor aqueous solubility of the nutraceutical compound pterostilbene.

EXPERIMENTAL METHODS

Reagents. Pterostilbene was acquired from Aptuit Laurus Ltd., India. Piperazine and glutaric acid were purchased from Sigma-Aldrich and used as received. All other chemicals were purchased from various suppliers and used without further purification.

Pterostilbene-Piperazine, 1. Cocrystal **1** was prepared by liquid-assisted grinding (LAG), solvent evaporation, or slow cooling. Under LAG conditions, a 2:1 mixture of pterostilbene (~65 mg, ~0.25 mmol) and piperazine (~11 mg, ~0.13 mmol) was added to an agate mill. Approximately 10 μL of solvent (ethanol or nitromethane) was added, and the material was ground for 20 min at a rate of 30 Hz. Single crystals were grown by slow evaporation of a 1:1 mixture of pterostilbene (135.2 mg, 0.53 mmol) and piperazine (45.5 mg, 0.53 mmol) in ethanol (2 mL). After 1 day, rod-shaped crystals were harvested. The material was scaled up by dissolution of pterostilbene (5.12 g, 20.0 mmol) and piperazine (862 mg, 10.0 mmol) in ethanol (~70 mL) with heat. The homogeneous solution was stirred in an oil bath for approximately 1 h, after which time the heat was removed and the solids were precipitated. The white crystalline solid was filtered and dried, yielding 10.54 g, 88%, of **1**.

Pterostilbene-Glutaric Acid, 2. Cocrystal **2** was also prepared by LAG, solvent evaporation, or slow cooling. Under LAG conditions, a 1:1 mixture of pterostilbene (~36 mg, ~0.14 mmol) and glutaric acid (~19 mg, ~0.14 mmol) was added to an agate mill. Approximately 10 μL of solvent (toluene or 2-propanol) was added, and the material was ground for 20 min at a rate of 30 Hz. Single crystals were grown by slow evaporation of a 1:1 mixture of pterostilbene (25.0 mg, 0.10 mmol) and glutaric acid (13.1 mg, 0.10 mmol) in toluene (3 mL). After 1 day, plate-shaped crystals were harvested. The material was scaled up by dissolution of pterostilbene (3.03 g, 11.8 mmol) and glutaric acid (1.55 g, 11.7 mmol) in toluene (~40 mL) with heat. The homogeneous solution was stirred, and upon cooling the solids precipitated. The white crystalline solid was filtered and dried, yielding 3.79 g, 83%, of **2**.

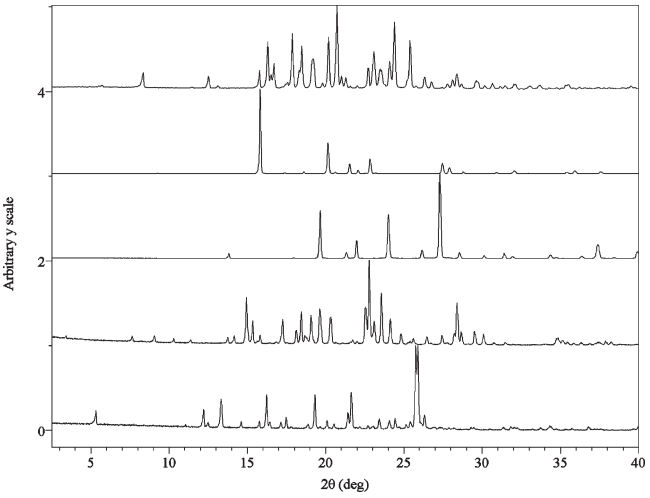

Figure 1. X-ray powder patterns of pterostilbene form I, piperazine (as received), glutaric acid (as received), **1**, and **2** (top to bottom).[15]

General Methods. *High-Throughput Screening (HTS).* Specified amounts of filtered 0.1 M pterostilbene solutions were dispensed into the wells of a 96-well microplate using the Symyx CORE(X). Stoichiometric amounts of several pharmaceutically acceptable or GRAS-listed carboxylic acid coformer stock solutions were added to the wells (~1−2 mg per well). Four different experiment types were conducted: slow evaporation, fast evaporation, sonication followed by slow evaporation, and sonication followed by fast evaporation. Upon completion, each well was analyzed by XRPD.

Physical Stability. Physical stability was evaluated at approximately 40 °C in ambient RH, 60 °C in ambient RH, ambient temperature in 75% RH, ambient temperature in 98% RH, and 40 °C in 75% RH. XRPD was used to detect dissociation. Vials of each cocrystal **1** and **2** were subjected to each condition for durations of 2 weeks, 1 month, and 2 months. Upon completion of the duration allowed, the samples were immediately analyzed by XRPD.

Powder Dissolution Experiments. Concentration measurements were performed using ultraviolet (UV) spectroscopy on a Spectramax Microplate Reader. For pterostilbene, a standard curve was produced by serial dilutions; absorbance readings at 315 nm for pterostilbene were used to establish a linear regression. The small amount of methanol used to prepare pterostilbene standards did not cause shifting in the absorbance spectrum. The UV spectra for the cocrystal formers, glutaric acid and piperazine, do not overlap at 315 nm. Powder dissolution of cocrystal **1** was carried out such that an excess of solid material was slurried in water at ambient conditions, and aliquots were taken at specific time points to derive a concentration versus time profile to estimate the maximum concentration before transformation to pterostilbene occurred. Aliquots were centrifuged, supernatant was extracted, and appropriate dilutions were made to maintain absorbance readings within the standard curve. Absorbance measurements were taken at 315 nm for pterostilbene, and concentrations were calculated from the standard curve. All experiments were repeated three times to evaluate the standard deviation. Particle size was not controlled for the powder dissolution experiments because the maximum concentration was sustained for several hours, and an initial dissolution rate, a property that would be directly affected by particle size, was not calculated from the data collected.

Powder dissolution of cocrystal **2** was attempted under the same experimental conditions as cocrystal **1**. However, XRPD results indicate the presence of crystalline pterostilbene after 5 min when the cocrystal was slurried in water at ambient conditions. Intrinsic dissolution in 900 mL of

Table 1. Crystal Data for Cocrystals 1 and 2

cocrystal	**1**	**2**
empirical formula	$C_{36}H_{42}N_2O_6$	$C_{21}H_{24}O_7$
MW	598.72	388.40
crystal syst	orthorhombic	monoclinic
space group, Z	$P2_12_12_1$, 4	$P2_1/c$, 4
a, Å	5.2586(7)	7.2644(3)
b, Å	11.7922(14)	32.8801(16)
c, Å	51.155(7)	7.9819(4)
α, deg	90	90
β, deg	90	96.000(2)
γ, deg	90	90
vol, Å^3	3172.2(7)	1896.07(15)
density, g/cm^3	1.254	1.361
temp, K	296	120(2)
X-ray wavelength	0.71073	0.71073
μ, mm^{-1}	0.085	0.102
F(000)	1280	724
Θ_{min}, deg	1.77	1.24
Θ_{max}, deg	27.57	32.58
reflns		
collected	37364	30177
independent	4250	6677
observed	1843	5136
threshold expression	>2$\sigma(I)$	>2$\sigma(I)$
R_1 (observed)	0.0545	0.0472
wR_2 (all)	0.1255	0.1396

water under ambient conditions was also attempted. However, XRPD results indicate precipitation of crystalline pterostilbene on the surface of the pellet after 30 min. Therefore, a concentration vs time profile and intrinsic dissolution rate value were unobtainable under these conditions.

Analytical Characterization. *X-ray Powder Diffraction (XRPD).* Patterns were collected using a PANalytical X'Pert Pro or Inel XRG-3000 diffractometer. An incident beam of Cu Kα radiation was produced using an Optix long, fine-focus source. PANalytical data were collected and analyzed using X'Pert Pro Data Collector software (v. 2.2b). Prior to the analysis a silicon specimen (NIST standard reference material 640c) was analyzed to verify the accuracy of the diffractometer optics using the known silicon 111 peak position at 28.441 °2θ to within ±0.01°. PANalytical diffraction patterns were collected using a scanning position-sensitive detector (X'Celerator) located 240 mm from the specimen.

Single-Crystal X-ray Diffraction (SCXRD). Data sets were collected on a Bruker SMART APEX II diffractometer using Mo Kα radiation. Data were collected using APEXII software.[12] Initial cell constants were found by small widely separated "matrix" runs. Data collection strategies were determined using COSMO. Scan speed and scan width were chosen based on scattering power and peak rocking curves. Temperature control for cocrystal **2** was provided with an Oxford Cryostream low-temperature device.

Unit cell constants and orientation matrix were improved by least-squares refinement of reflections thresholded from the entire data set. Integration was performed with SAINT,[13] using this improved unit cell as a starting point. Precise unit cell constants were calculated in SAINT from the final merged data set. Lorenz and polarization corrections were applied. Where indicated, absorption corrections were made using the multiscan procedure in SADABS.

Data were reduced with SHELXTL.[14] The structures were solved in all cases by direct methods without incident. Absorption correction was not applied (maximum $\mu d \approx 0.03$ in both cases).

Table 2. Hydrogen-Bond Geometries for Cocrystals 1 and 2

cocrystal	D−H···A	d(H···A), Å	d(D···A), Å	θ(DHA), deg
1	O211−H211···N11	1.87(4)	2.711(5)	160(4)
	O212−H212···N14	1.82(5)	2.746(5)	166(4)
	N11−H11···O211#1	2.35(4)	3.224(5)	168(4)
	N14−H14···O212#2	2.60(5)	3.338(5)	173(5)
2	O11−H11···O21	1.821(17)	2.6798(12)	170.9(16)
	O15−H15···O16	1.792(17)	2.6463(12)	173.5(16)
	O21−H21···O12	1.850(19)	2.7001(12)	173.7(16)

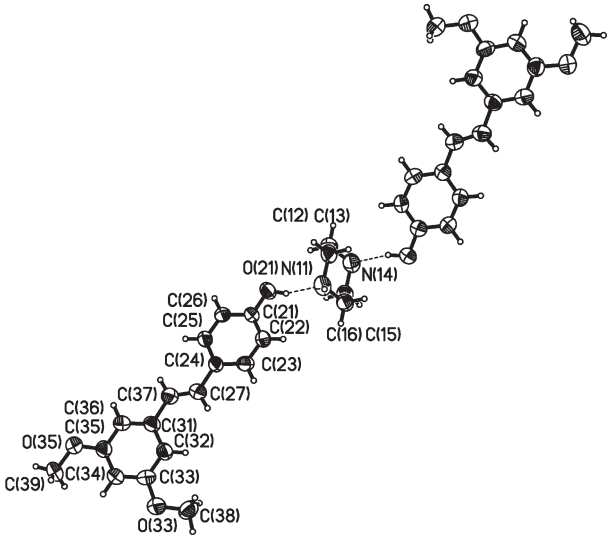

Figure 2. Labeled thermal ellipsoids plot (displayed at a 50% probability level) of the 2:1 pterostilbene-piperazine cocrystal **1**.

Cocrystal ***1***. The two crystallographically nonequivalent pterostilbenes were distinguished with use of the SHELXL "RESI" command. The compound crystallizes in the noncentrosymmetric space group $P2_12_12_1$. Due to the absence of heavy atom anomalous scatterers, determination of crystal handedness was not pursued, and Friedel opposites were merged. Coordinates for the amine protons H11 and H14 and phenol protons H21 (on each pterostilbene) were allowed to refine. An extinction correction was applied; the EXTI parameter refined to a small but nonzero number.

Cocrystal ***2***. Coordinates for the carboxylic acid protons H11 and H15 and the phenol proton H21 were allowed to refine.

RESULTS AND DISCUSSION

Cocrystals **1** and **2** were synthesized through a variety of different reaction conditions: liquid-assisted grinding (LAG), slow evaporation, and slow cooling. Evidence of cocrystal **2** was first observed through HTS experiments where a unique XRPD pattern was detected in wells containing glutaric acid. Initial characterization by XRPD of cocrystals **1** and **2** displayed unique patterns in comparison to pterostilbene, piperazine, or glutaric acid, Figure 1. Proton NMR revealed the 2:1 and 1:1 pterostilbene/coformer stoichiometries for cocrystals **1** and **2**, respectively, while the TGA thermograms showed negligible weight loss until decomposition; thus the cocrystals were characterized as nonsolvated/hydrated.

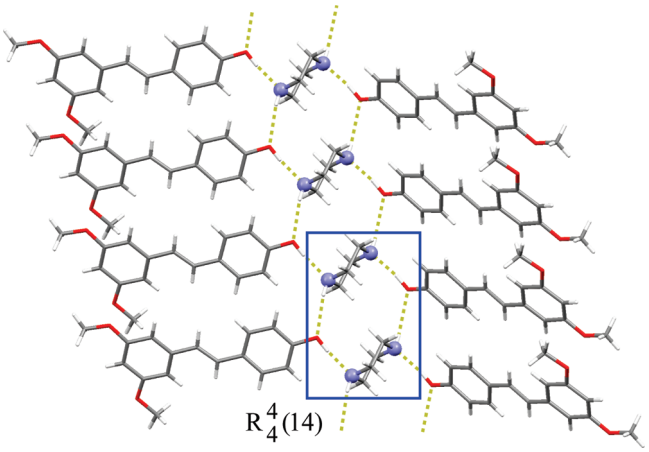

Figure 3. Extended architecture displaying the hydrogen bond donor/acceptor ability of piperazine in cocrystal **1**.[16] The nitrogen atoms on piperazine are highlighted as blue spheres while the hydrogen bonds are yellow dashed lines.

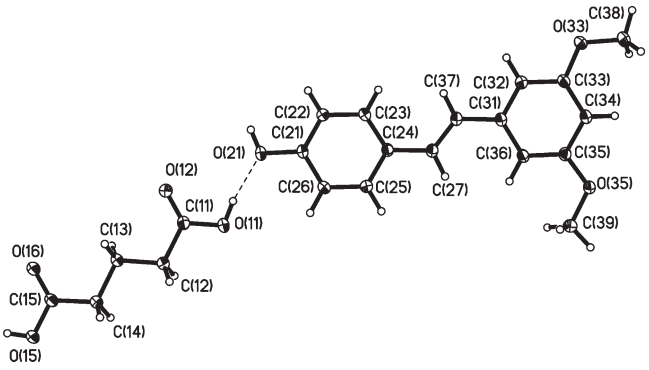

Figure 4. Labeled thermal ellipsoids plot (displayed at a 50% probability level) of the 1:1 pterostilbene-glutaric acid cocrystal **2**.

Single crystals of cocrystals **1** and **2** were generated by slow evaporation techniques from ethanol and toluene, respectively. After 1 day, crystals suitable for single-crystal X-ray diffraction were culled from the mother liquors.

Cocrystal **1** crystallizes in the orthorhombic space group $P2_12_12_1$, Table 1. The asymmetric unit of cocrystal **1** contains two pterostilbene molecules and one piperazine, linked through O−H···N hydrogen bonds (Table 2) from the hydroxy moiety of pterostilbene to the nitrogen atom of piperazine, Figure 2. The three-component supermolecules are cross-linked into one-dimensional rows through N−H···O hydrogen bonds from the N−H of piperazine to the oxygen atom of the pterostilbene molecule resulting in a $R_4^4(14)$ graph set notation, Figure 3.

Thirteen hydrogen-bonded (and two halogen-bonded) cocrystals exist in the CSD with piperazine, showing its ability to form neutral multicomponent crystals with a broad range of functional groups.[17] Additionally, the same $R_4^4(14)$ graph set observed in cocrystal **1** occurs when piperazine is cocrystallized with paracetamol[18] or 6-bromo-2-naphthol;[19] however, each of the other 11 hydrogen-bonded structures displays a different set of connectivities and hydrogen bonding motifs.

Cocrystal **2** crystallizes in the monoclinic space group $P2_1/c$, Table 1. The asymmetric unit of cocrystal **2** contains one pterostilbene and one glutaric acid molecule, Figure 4.

One carboxylic acid moiety of glutaric acid forms an O−H···O hydrogen bond to the hydroxyl oxygen of pterostilbene, while the second acid moiety forms an acid−acid dimer with a neighboring pterostilbene−carboxylic acid pair, generating a four-component supramolecular assembly, Figure 5. Extension of the structure reveals an additional series of O−H···O (O−H···$O_{carbonyl}$ and O−H···$O_{hydroxyl}$) hydrogen bonds linking the individual assemblies together. Overall, two primary hydrogen-bonding synthons are located within the structure and can easily be described through graph set notations:[20] the conventional $R_2^2(8)$ acid−acid dimer and a $R_4^4(12)$ hydroxyl−carbonyl/hydroxyl−hydroxyl motif. A search of the CSD revealed that the $R_2^2(8)$ graph set (acid−acid dimer) is common place (2991 hits); however, the $R_4^4(12)$ graph set (hydroxyl−carbonyl/hydroxyl−hydroxyl motif) occurs less frequently (107 hits).

Two pharmaceutical properties of cocrystals **1** and **2** were evaluated and measured: physical stability with respect to temperature and relative humidity (RH) and aqueous dissolution.

Stability testing is an integral part of the drug development process. Early in development, stability testing (normal and accelerated) on new chemical entities is required to help select the most satisfactory form with the desired pharmaceutical profile. Stability studies as a function of time versus humidity and temperature are particularly useful in assessing the shelf life, expiry date, storage conditions, and packaging required for an API and drug product. Thus, both cocrystals **1** and **2** were subjected to a range of different humidities and temperatures for 2 weeks, 1 month, and 2 months. At each time point, the materials were analyzed by XRPD to determine whether the cocrystals displayed physical instability in the presence of increased temperature or humidity by comparison to the XRPD pattern of the unstressed cocrystal. No additional analysis was conducted to assess the chemical stability of either cocrystal **1** or **2**. Both cocrystals displayed remarkable physical stability, with no dissociation or recrystallization based on no observable differences in the XRPD patterns in comparison to the unstressed materials after 2 weeks, 1 month, and 2 months of accelerated stress under the following conditions: 40 °C/ambient RH, 60 °C/ambient RH, ambient temperature/75% RH, ambient temperature/98% RH, and 40 °C/75% RH.

Both piperazine and glutaric acid are freely soluble in aqueous media with estimates of approximately 150 and 850 mg/mL, respectively.[21] Thus, due to their high water solubility, we anticipated that the aqueous dissolution of the pterostilbene cocrystals would increase in comparison to pterostilbene. Slurrying cocrystal **1** in water at ambient temperature for approximately 1 day resulted in material that was characterized by XRPD to be a physical mixture of cocrystal **1** and Form I of pterostilbene. Therefore aliquots were taken for approximately 5 hours to generate a concentration versus time profile (Figure 6). The concentration of pterostilbene from the dissolution of cocrystal **1** was measured to be approximately 6 times higher than that of Form I of pterostilbene after approximately 5 hours. Although XRPD results indicate partial transformation of cocrystal **1** to Form I of pterostilbene after 5 hours, the concentration of pterostilbene was maintained as a plateau over the course of the powder dissolution experiment. This sustained increase in pterostilbene concentration for cocrystal **1** is similar to that observed for the pterostilbene-caffeine cocrystal.[9] Solution complexation between pterostilbene and piperazine may exist and is likely aiding in the sustained solution concentrations for cocrystal **1**.

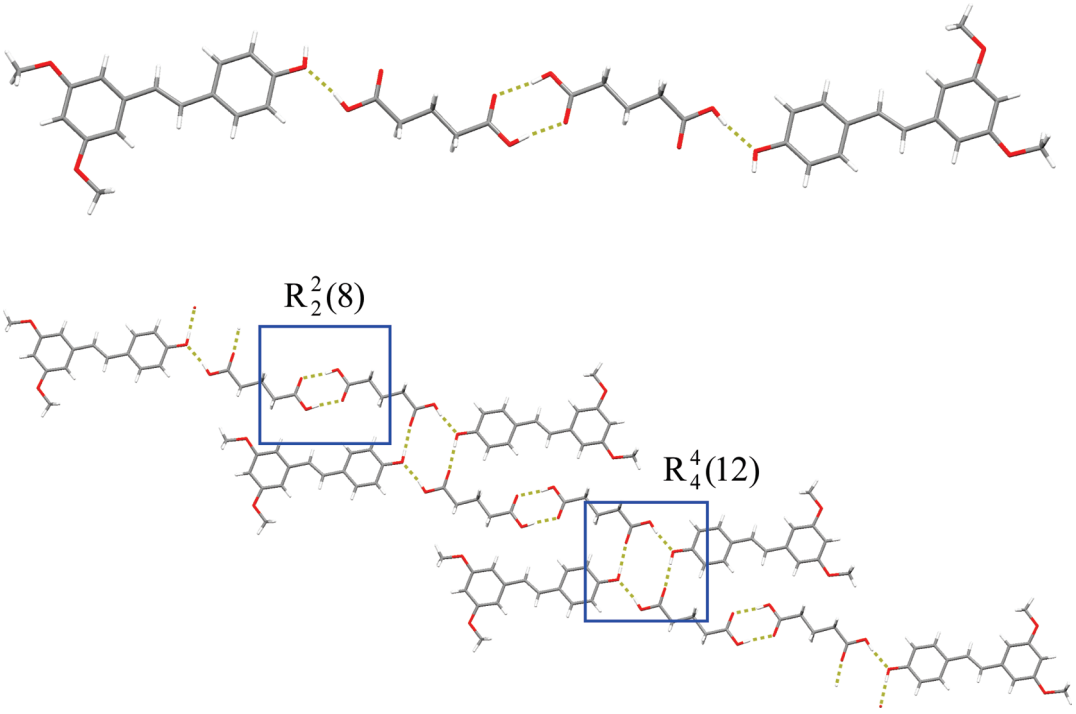

Figure 5. The 1:1 four-component supramolecular assembly between glutaric acid and pterostilbene, cocrystal **2** (top) and extended architecture displaying the graph-set notations of the two different hydrogen-bonded synthons within the structure (bottom).

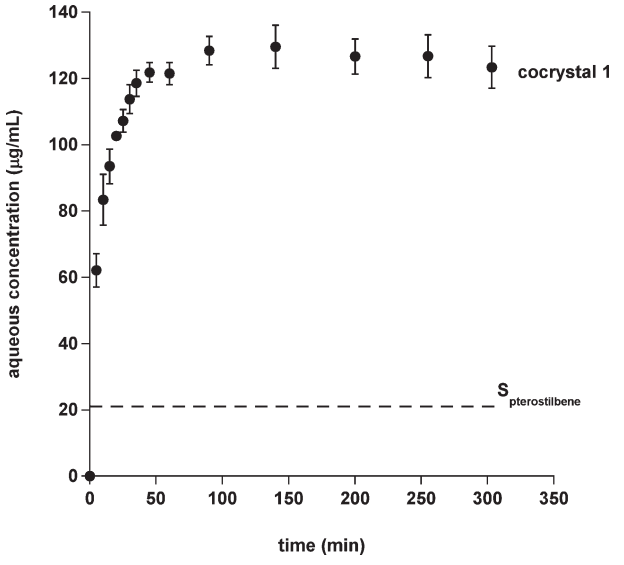

Figure 6. Concentration vs time profile for cocrystal **1** and equilibrium solubility of pterostilbene at ambient temperature.

Precipitation of pterostilbene was observed within 5 minutes upon slurrying of cocrystal **2** in water at ambient temperature. Therefore, it can be assumed that the kinetic solubility of cocrystal **2** is higher than the solubility of pterostilbene, but due to rapid precipitation of pterostilbene, a quantitative assessment of the concentration increase was not attainable. Interestingly, cocrystal **2** remained in tact (i.e., did not dissociate) upon exposure to 98% relative humidity at ambient temperature, suggesting that water vapor does not lower the activation barrier enough to cause dissociation. Stirring cocrystal **2** in an aqueous slurry sufficiently lowers the activation barrier to cause dissociation followed by rapid precipitation of pterostilbene likely because little or no complexation between pterostilbene and glutaric acid exists in solution.

As was demonstrated from our previous studies,[9] pterostilbene can act as a coformer to form cocrystals with caffeine and carbamazepine; while in this work, pterostilbene was selected as an API in the formation of cocrystals with pharmaceutically acceptable coformers, glutaric acid and piperazine. These cocrystal examples provide cases where the classification or label of the components (API or coformer) is not critical, and the cocrystal structure and properties are not affected by the nomenclature of choice. Whether pterostilbene was treated as an API or a coformer, the main observation is that the concentration of pterostilbene in solution, measured from the different cocrystals, varied greatly.

It is noted that the dissolution and solubility of the caffeine and carbamazepine cocrystals presented earlier[9] were monitored by measuring the UV spectrum of the respective components rather than that of pterostilbene. For these 1:1 mole ratio cocrystals, the concentration of caffeine or carbamazepine is directly proportional to the concentration of pterostilbene (i.e., as one mole of cocrystal dissolves, one mole of both components are released to the solution). Therefore, monitoring either component by UV−vis spectroscopy can be done so long as the cocrystal remains intact, as was observed for these two cocrystals over the course of the results presented. For the piperazine cocrystal, dissociation and precipitation of pterostilbene was observed within the course of the experiment according to XRPD results; thus the absorbance of pterostilbene was monitored to provide an accurate representation of the solution concentration of pterostilbene. Monitoring the absorbance of piperazine may have resulted in misleading results since the cocrystal was observed to dissociate and pterostilbene was found to precipitate during the dissolution study.

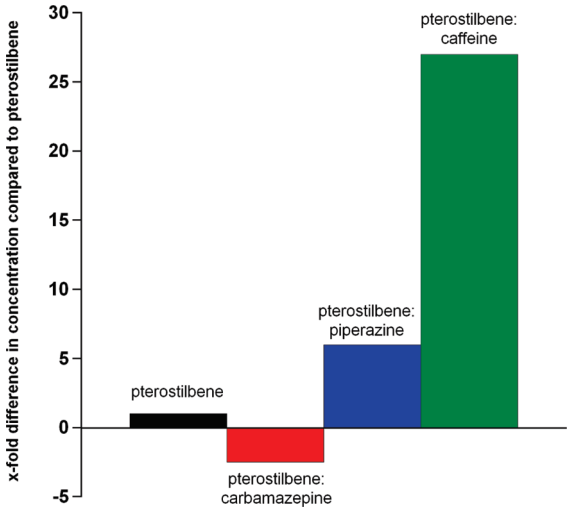

Figure 7. Comparison between the aqueous solubility of pterostilbene and the solution concentration of pterostilbene achieved from three cocrystals. The *x*-fold increase or decrease is calculated from equilibrium or kinetic solubility measured for the respective cocrystal. Pterostilbene solubility (black) is represented as one.

Figure 7 shows the increase or decrease in pterostilbene solution concentration that resulted from the three cocrystals. The cocrystal of pterostilbene with carbamazepine in fact decreased the overall solution concentration of pterostilbene nearly 3-fold, while cocrystals with piperazine and caffeine achieved 6- and 27-fold increases in solution concentration of pterostilbene, respectively.

CONCLUSIONS

Within this study, we successfully cocrystallized pterostilbene with piperazine and glutaric acid, showing the ability of pterostilbene to form cocrystals with pharmaceutically acceptable coformers. Both cocrystals displayed remarkable physical stability, with respect to RH and temperature over specified time periods of up to 8 weeks. Dissolution of cocrystal **2** resulted in rapid precipitation of pterostilbene, and thus measurement of the increase in pterostilbene concentration was unattainable. However, the aqueous solution concentration was measured for cocrystal **1** revealing a 6-fold increase in pterostilbene concentration compared with the solubility of pterostilbene. Cocrystals that result in an increased solution concentration of an API or nutraceutical compound, such as pterostilbene, could lead to enhanced pharmacological properties, particularly when the concentration is sustained for several hours.

ASSOCIATED CONTENT

Supporting Information. Simulated and experimental XRPD patterns of cocrystals **1** and **2**, XRPD patterns after temperature or %RH stress experiments, XRPD patterns after solubility experiments, and crystallographic information files for **1** and **2**. This material is available free of charge via the Internet at http://pubs.acs.org.

AUTHOR INFORMATION

Corresponding Author

*E-mail: sarah.bethune@aptuit.com. Phone: 1-765-463-0112.

Present Addresses

†Halliburton, 2600 South 2nd Street, Duncan, OK 73536, USA.

ACKNOWLEDGMENT

We thank Dr. John Depser for single-crystal data collection and structure solution of **1** and **2**, Mr. Rex Shipplett for well-plate screening experiments, and SSCI's analytical services for data collection. We also thank Mr. Eyal Barash, Dr. David Engers, and Ms. Melanie Roe for careful review of the manuscript.

REFERENCES

(1) A "nutraceutical" compound can be defined as, "a food (or part of a food) that provides medical or health benefits, including the prevention and/or treatment of a disease and possesses a physiological benefit or reduces the risk of chronic disease".Kalra, E. K. *AAPS Pharm. Sci.* **2003**, *3*, No. 25.

(2) (a) Rimando, A. M.; Kalt, W.; Magee, J. B.; Dewey, J.; Ballington, J. R. *J. Agric. Food Chem.* **2004**, *52*, 4713–4719. (b) Adrian, M.; Jeandet, P.; Douillet-Breuil, A. C.; Tesson, L.; Bessis, R. *J. Agric. Food Chem.* **2002**, *48*, 6103–6105. (c) Langcake, P. *Physiol. Plant Pathol.* **1981**, *18*, 213–226.

(3) (a) Rimando, A. M.; Cuendet, M.; Desmarchelier, C.; Mehta, R. G.; Pezzuto, J. M.; Duke, S. O. *J. Agric. Food Chem.* **2002**, *50*, 3453–3457. (b) Cichocki, M.; Paluszczak, J.; Szaefer, H.; Piechowiak, A.; Rimando, A. M.; Baer-Dubowska, W. *Mol. Nutr. Food Res.* **2008**, *52*, 62–70. (c) Suh, N.; Paul, S.; Hao, X.; Simi, B.; Xiao, H.; Rimando, A. M.; Reddy, B. S. *Clin. Cancer Res.* **2007**, *13*, 350–355.

(4) (a) Lin, H.-S.; Yue, B.-D.; Ho, P. C. *Biomed. Chromatogr.* **2009**, *23*, 1308–1315. (b) Das, S.; Lin, H.-S.; Ho, P. C.; Ng, K.-Y. *Pharm. Res.* **2008**, *25*, 2593–2600.

(5) Ivanisevic, I.; Andres, M. C.; Stephens, K.; Bethune, S.; Bower, M.; Wolfe, S.; Smit, J.; Gilkinson, A.; Roe, M. manuscript in preparation, 2011.

(6) (a) Etter, M. C. *Acc. Chem. Res.* **1990**, *23*, 120–126. (b) Aakeröy, C. B.; Salmon, D. J. *CrystEngComm* **2005**, *7*, 439–448. (c) MacGillivray, L. *CrystEngComm* **2004**, *6*, 77–78. (d) Desiraju, G. R. *Acc. Chem. Res.* **2002**, *35*, 565–573. (e) Moulton, B.; Zaworotko, M. *Chem. Rev.* **2001**, *101*, 1629–1658. (f) Lehn, J.–M. *Science* **2002**, *295*, 2400–2403. (f) Grepioni, F.; Braga, D. *Making Crystals by Design—From Molecules to Molecular Materials, Methods, Techniques, Applications*; Wiley-VCH: Weinheim, Germany, 2007; Chapter 2.5 and references therein.

(7) (a) Crystal Growth and Design virtual issue on Pharmaceutical Cocrystals, http://pubs.acs.org/page/cgdefu/vi/1, and references therein. (b) Good, D. J.; Rodríguez-Hornedo, N. *Cryst. Growth Des.* **2009**, *9* (5), 2252–2264. (c) Childs, S. L.; Chyall, L. J.; Dunlap, J. T.; Smolenskaya, V. N.; Stahly, B. C.; Stahly, G. P. *J. Am. Chem. Soc.* **2004**, *126*, 13335–13342. (d) Shiraki, K.; Takata, N.; Takano, R.; Hayashi, Y.; Terada, K. *Pharm. Res.* **2008**, *25*, 2581–2592.

(8) Childs, S. L.; R.odríguez-Hornedo, N.; Reddy, L. S.; Jayasankar, A.; Maheshwari, C.; McCausland, L.; Shipplett, R.; Stahly, B. C. *CrystEngComm* **2008**, *10*, 856–864.

(9) Schultheiss, N.; Bethune, S.; Henck, J. O. *CrystEngComm* **2010**, *12*, 2436–2442.

(10) Coformers were selected for the screen if they possessed estimated aqueous solubilities of 30 mg/mL or greater.

(11) (a) *Handbook of Pharmaceutical Salts: Properties, Selection and Use*; Stahl, P. H., Wermuth, C. G., Eds.; Verlag Helvetica Chimica Acta: Zürich, 2002. (b) Generally Regarded as Safe: http://www.cfsan.fda.gov/~rdb/opa-gras.html and http://www.cfsan.fda.gov/~dms/grasguid.html (c) Everything Added to Food Stuff in the United States: Http://vm.cfsan.fda.gov/~dms/eafus.html.

(12) *APEXII*, v1.27; Bruker Analytical X-ray Systems, Madison, WI, 2005.

(13) *SAINT*, v6.02; Bruker Analytical X-ray Systems, Madison, WI, 1997–1999.

(14) *SHELXTL*, v5.10; Bruker Analytical X-ray Systems, Madison, WI, 1997.
(15) Figure generated using proprietary in-house Pattern Match software:Ivanisevic, I.; Bugay, D. E.; Bates, S. *J. Phys. Chem. B* **2005**, *109*, 7781–7787.
(16) Images created using Mercury 2.1.
(17) CSD refcodes: AYISIK, DIVCUH, DIVDOC, DOSJOK, FEKQOC, HIBFED, JESMEA, LAKMOA, LOHNOM, MUPPUI, OGEZIJ, QAMRAY, RAWFAW, TICFOA, and XOKBOO.
(18) Oswald, I. D. H.; Allan, D. R.; McGregor, P. A.; Motherwell, W. D. S.; Parsons, S.; Pulham, C. R. *Acta Crystallogr.* **2002**, *B58*, 1057–1066.
(19) Tian, Y.; Cui, D. *Acta Crystallogr.* **2008**, *E64*, 2334–2335.
(20) Etter, M. C.; MacDonald, J. C.; Bernstein, J. *Acta Crystallogr.* **1990**, *B46*, 256–262.
(21) Approximate aqueous solubilities were calculated based on the total solvent used to produce a solution; actual solubilities may be greater due to the slow rate of dissolution.